

Catalytic Mechanism and Product Specificities of Protein Arginine Methyltransferase PRMT7: A Study from QM/MM molecular dynamics and free energy simulations

Wan-Sheng Ren^{‡,1}, Kai-Bin Jiang^{‡,1,‡}, Hao Deng¹, Nan Lu¹, Tao Yu^{*,2}, Hong Guo^{*,3},
Ping Qian^{*,1}

¹ *Chemistry and Material Science Faculty, Shandong Agricultural University, Taian 271018, P. R. China*

² *Department of Chemistry, University of North Dakota, Grand Forks, ND 58202-9024, United States*

³ *Department of Biochemistry and Cellular and Molecular Biology, University of Tennessee, Knoxville, TN 37996, United States UT/ORNL Center for Molecular Biophysics, Oak Ridge National Laboratory, Oak Ridge, TN 37830, United States*

[‡] These authors contributed equally to this work.

[‡] Current Address: State Key Laboratory of Structural Chemistry, Fujian Institute of Research on the Structure of Matter, Chinese Academy of Sciences, 350002, P. R. China.

* Corresponding authors: Tel.: +86 538 8241175; fax: +86 538 8242251.

E-mail address: qianp@sdau.edu.cn (to P. Qian), hguo1@utk.edu (to H. Guo) and tao.yu.1@und.edu (to T. Yu)

Supporting Information

Comparison of potential energy curves for the methyl transfer calculated from DFTB3, MP2/6-31G(d) and MP2/6-31G(d,p) in simplified cluster models

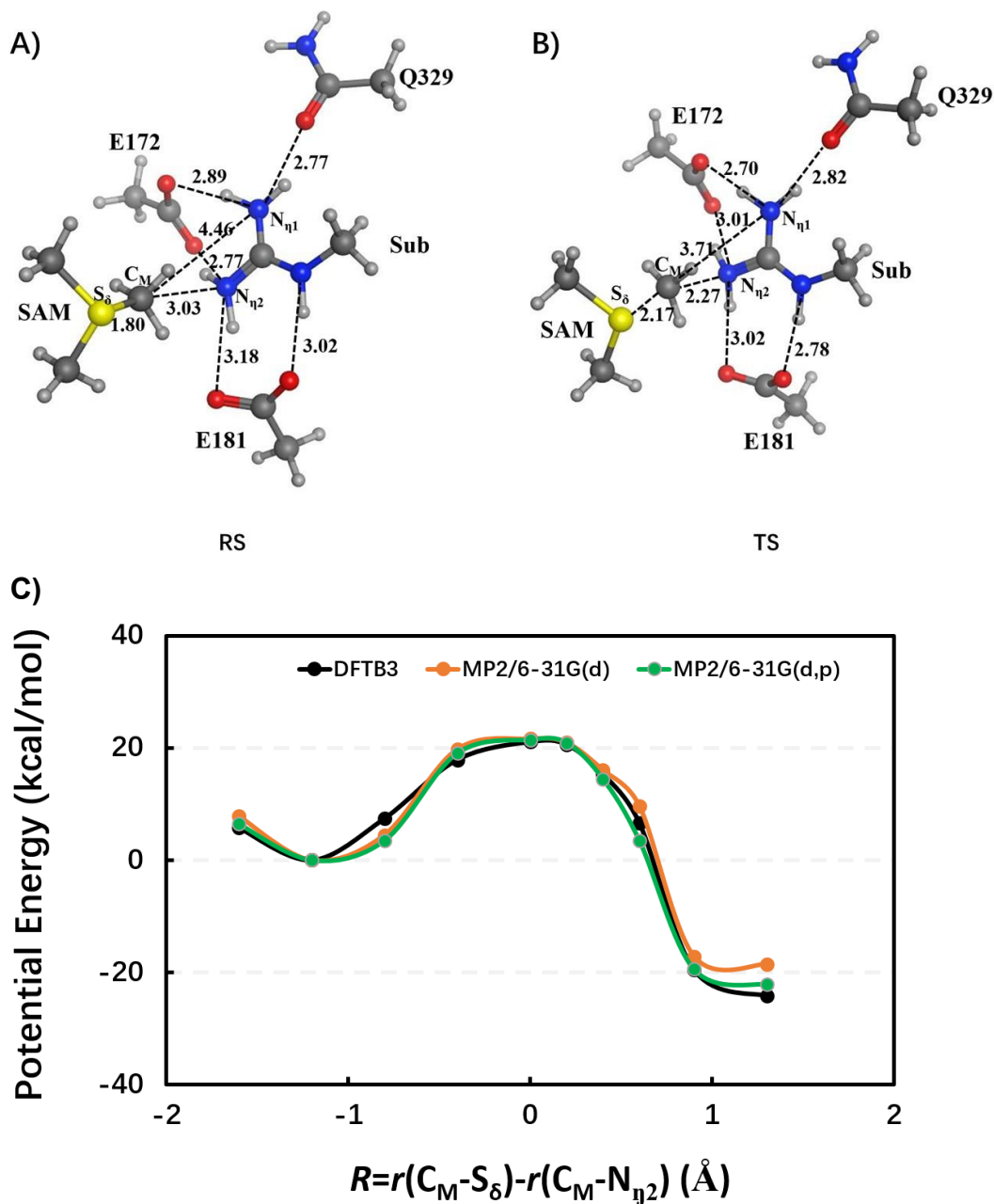


Figure S1. (A) The cluster model system for the reaction state (RS) of wild-type PRMT7 used for comparison the results of potential energy calculations from DFTB3, MP2/6-31G(d) and MP2/6-31G(d,p) calculations. The methyl group was transferred from the S_δ-atom to the guanidine N_{η2}-atom. (B) The structure near transition state (TS) for the methyl transfer. (C) Comparison of potential energy curves for the methyl transfer calculated from DFTB3, MP2/6-31G(d) and MP2/6-31G(d,p), respectively.

Comparison of the Mulliken charge distributions from the DFTB3/CHARMM calculations for guanidino group in wild-type PRMT7 and three mutants (E172Q, E181Q, Q329A) as well as Mulliken charge distributions from the HF/STO-3G calculations for guanidino group in four corresponding models

Table S1. Comparison of the Mulliken charge distributions (unit: e) of guanidino group in wild-type PRMT7 and three mutants based on the DFTB3/CHARMM calculations using typical structures of the wild-type and mutated enzymes obtained from the QM/MM MD simulations.

Molecular Label ^a	Atomic Label ^a	WT	E172Q	E181Q	Q329A
Sub	NE	-0.31290	-0.28172	-0.22043	-0.2659
	HE	0.30546	0.28319	0.24919	0.28652
	CZ	0.52443	0.49332	0.47848	0.52305
	N_{η1}	-0.43220	-0.40209	-0.44412	-0.44635
	HH11	0.25114	0.28364	0.34175	0.32138
	HH12	0.30188	0.27575	0.30072	0.23625
	N_{η2}	-0.51577	-0.38762	-0.45007	-0.50241
	HH21	0.27439	0.27219	0.29295	0.31202
	HH22	0.32841	0.30243	0.25216	0.28058
Guanidino group		0.72484	0.83909	0.80063	0.74514

Table S2. Comparison of the Mulliken charge distributions (unit: e) in four small model systems (see the structures in Figure S2) based on the HF/STO-3G calculations.

Molecular Label ^a	Atomic Label ^a	WT	E172Q	E181Q	Q329A	Molecular Label ^a	Atomic Label ^a	WT	E172Q	E181Q	Q329A
SAM	S ₈	0.493803	0.502782	0.531077	0.491074	Sub	N _{n1}	-0.44103	-0.415399	-0.428612	-0.441866
	C _M	-0.223326	-0.214754	-0.248886	-0.217716		HH11	0.290791	0.247571	0.30255	0.280349
	HM1	0.117354	0.139674	0.140417	0.139219		HH12	0.220625	0.255683	0.289871	0.223503
	HM2	0.165463	0.132322	0.140074	0.123448		N _{n2}	-0.451915	-0.425013	-0.430493	-0.452757
	HM3	0.140551	0.110346	0.134358	0.149334		HH21	0.26869	0.236899	0.309891	0.277465
	CG	-0.22792	-0.22026	-0.240321	-0.239485		HH22	0.25819	0.305989	0.221683	0.257363
	HG1	0.12633	0.145203	0.128426	0.12731		CZ	0.431032	0.451305	0.456944	0.436781
	HG2	0.123034	0.113907	0.126665	0.117441		NE	-0.365891	-0.349418	-0.345345	-0.363625
	HG3	0.11446	0.132871	0.14221	0.122798		HE	0.282187	0.291359	0.235998	0.29329
	C5'	-0.230397	-0.2352	-0.254022	-0.215606		CD	-0.067659	-0.064206	-0.06241	-0.06724
	H5'1	0.120141	0.138554	0.124464	0.113092		HD1	0.078034	0.065596	0.085845	0.062732
	H5'2	0.142819	0.120952	0.127732	0.152672		HD2	0.075806	0.072694	0.08996	0.070117
	H5'3	0.126262	0.132352	0.133563	0.120414		HD3	0.097543	0.10889	0.09718	0.112263
Sum		0.988574	0.998749	0.985757	0.983995	Sum		0.676403	0.78195	0.823062	0.688375
						Guanidine group		0.492679	0.598976	0.612487	0.510503

a) See the structure Figure S2.

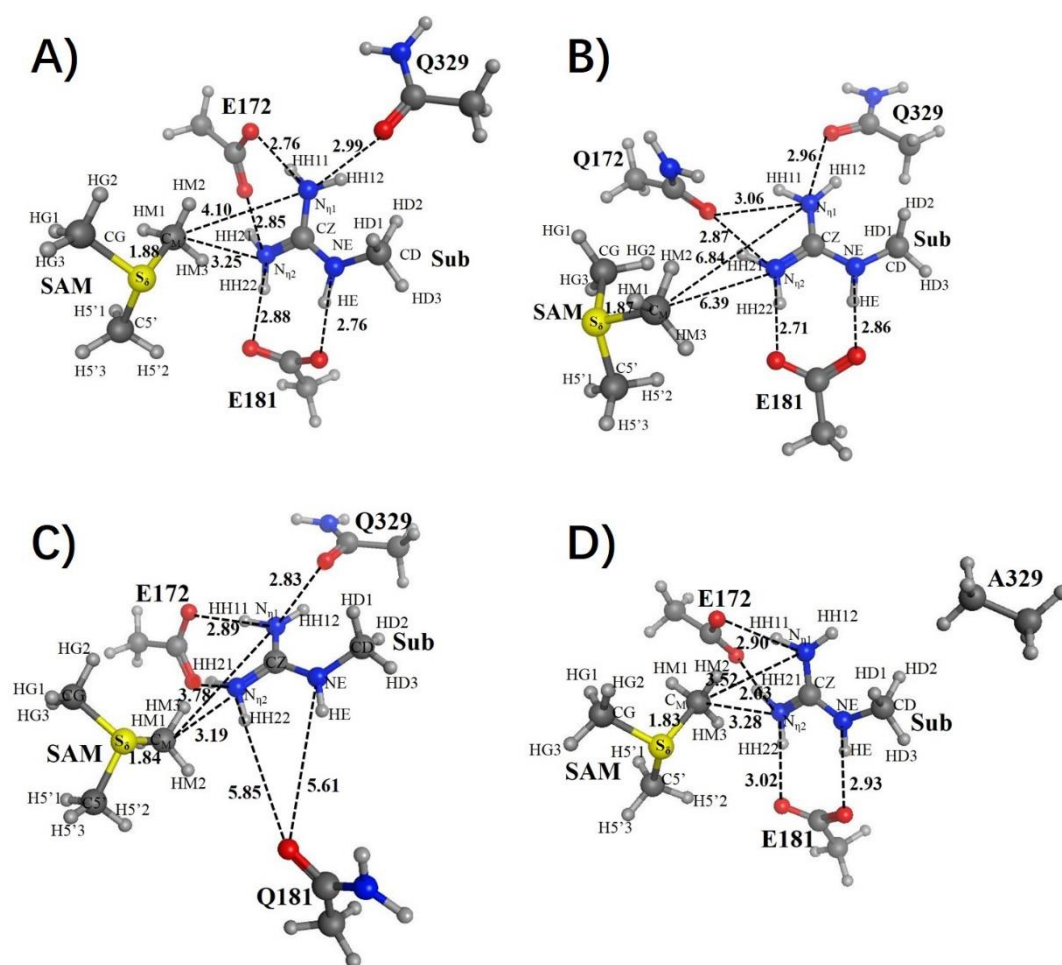


Figure S2. The cluster models of (A) wild-type PRMT7, (B) E172Q, (C) E181Q and (D) Q329A. For each cluster model, the representative active-site structures and key residues were based on the structures from QM/MM molecular dynamics simulations.

The representative active-site structures for the reactant state and near transition state as well as the free energy profiles for the 2nd methylations

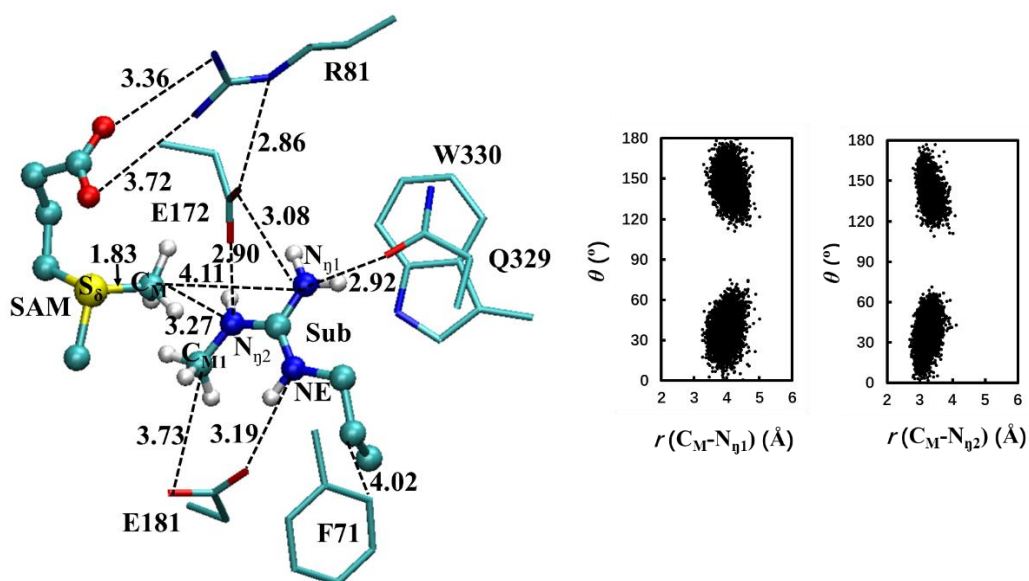


Figure S3. Representative active site structure of the reactant complex I for 2nd methylation along with $r(\text{C}_M\cdots\text{N}_\eta)$ and θ distributions obtained from the QM/MM simulation. (left) 2nd methylation on N_{η1}. (right) 2nd methylation on N_{η2}.

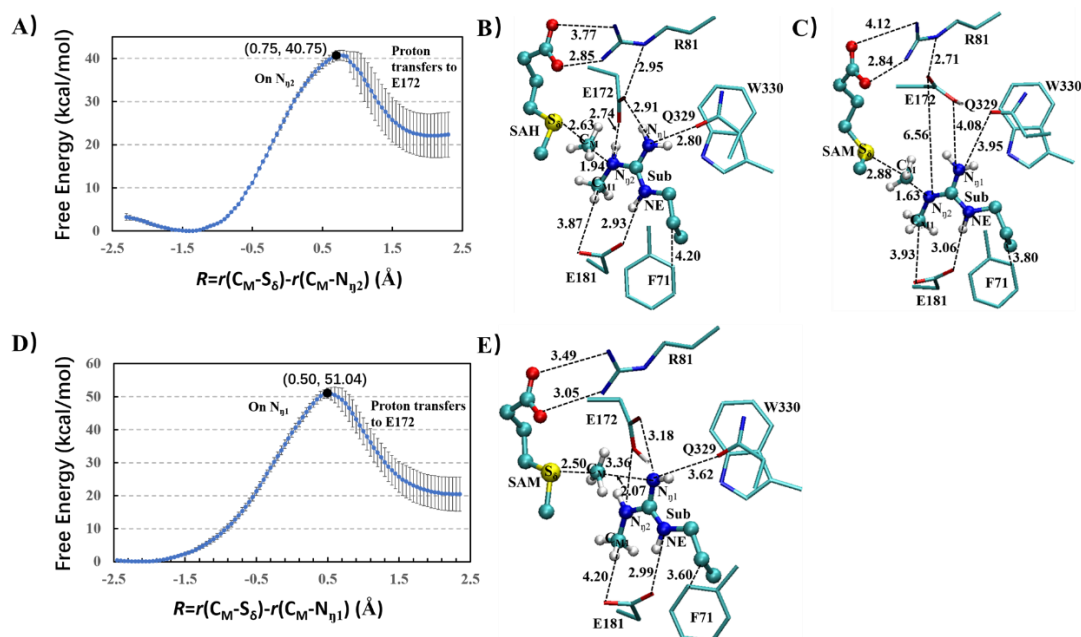


Figure S4. (A) Free energy profile for the 2nd methylation to N_{η2} in complex I. (B) Representative active site structures of near TS for the 2nd methylation to N_{η2} obtained from the free energy simulations. (C) Representative active site structures of (TS+1) state for the 2nd methylation to N_{η2} as well as the proton transfer to E172. (D) Free energy profile for the 2nd methylation to N_{η1}. (E) Representative active site structures of near TS for the 2nd methylation to N_{η1} as well as the proton transfer to E172.

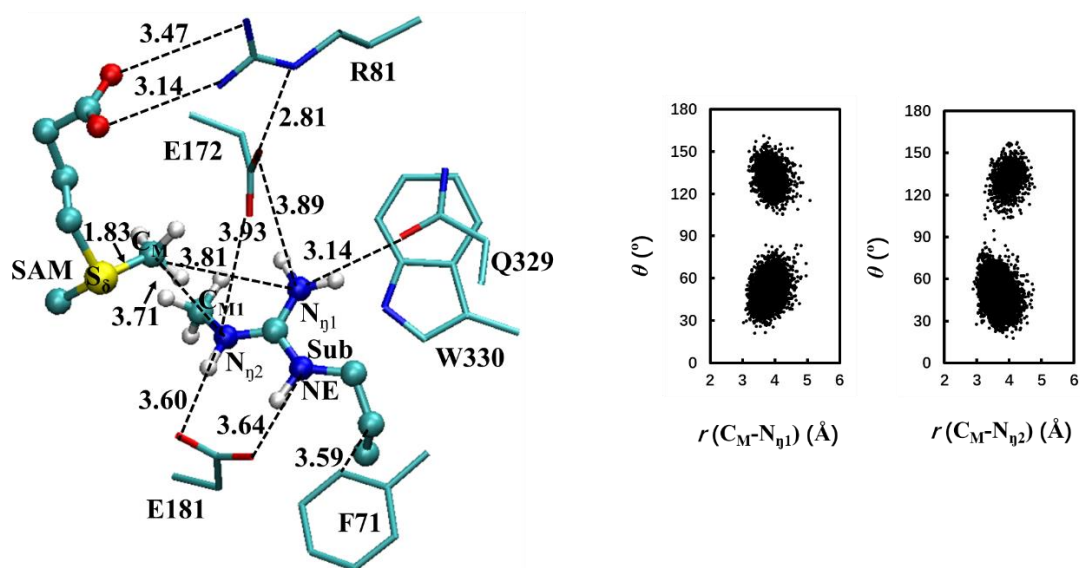


Figure S5. Representative active site structure of the reactant complex II for 2nd methylation along with $r(C_M \cdots N_{\eta})$ and θ distributions obtained from the QM/MM simulation. (left) 2nd methylation on N_{η1}. (right) 2nd methylation on N_{η2}.

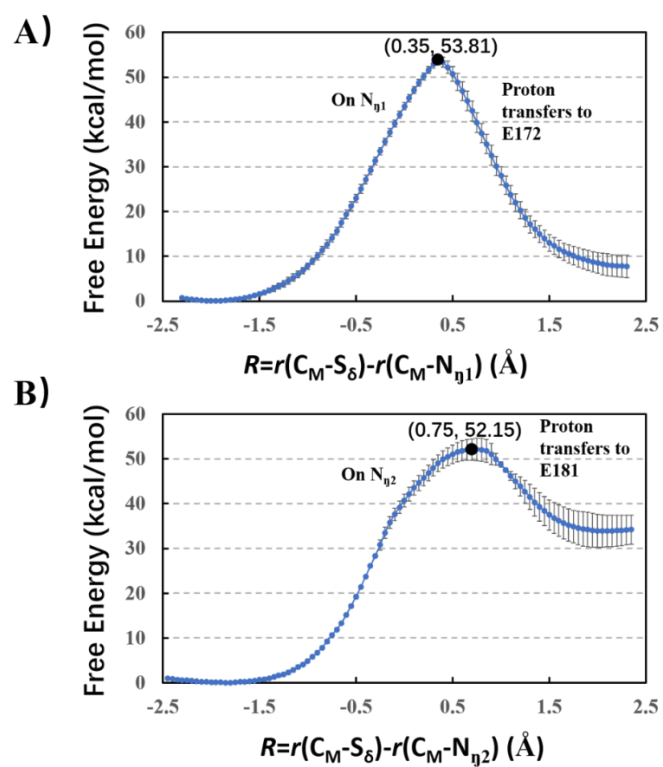


Figure S6. Free energy profile for the 2nd methylation addition to (A) the $N_{\eta 1}$ atom and (B) the $N_{\eta 2}$ atom in complex II.

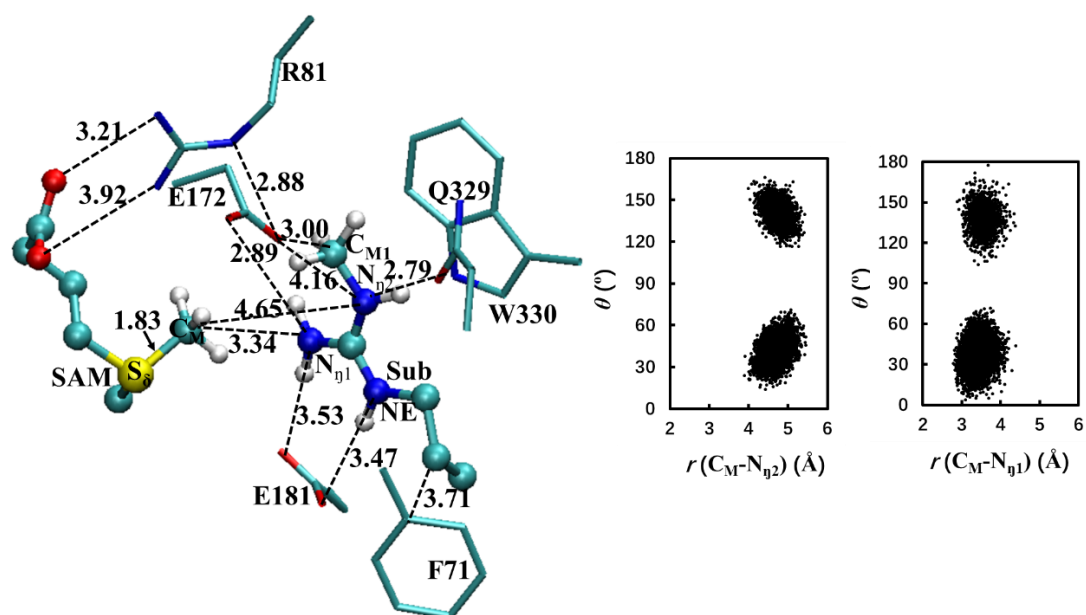


Figure S8. Representative active site structure of the reactant complex III for 2nd methylation along with $r(C_M \cdots N_\eta)$ and θ distributions obtained from the QM/MM simulation. (left) 2nd methylation on N_{η2}. (right) 2nd methylation on N_{η1}.

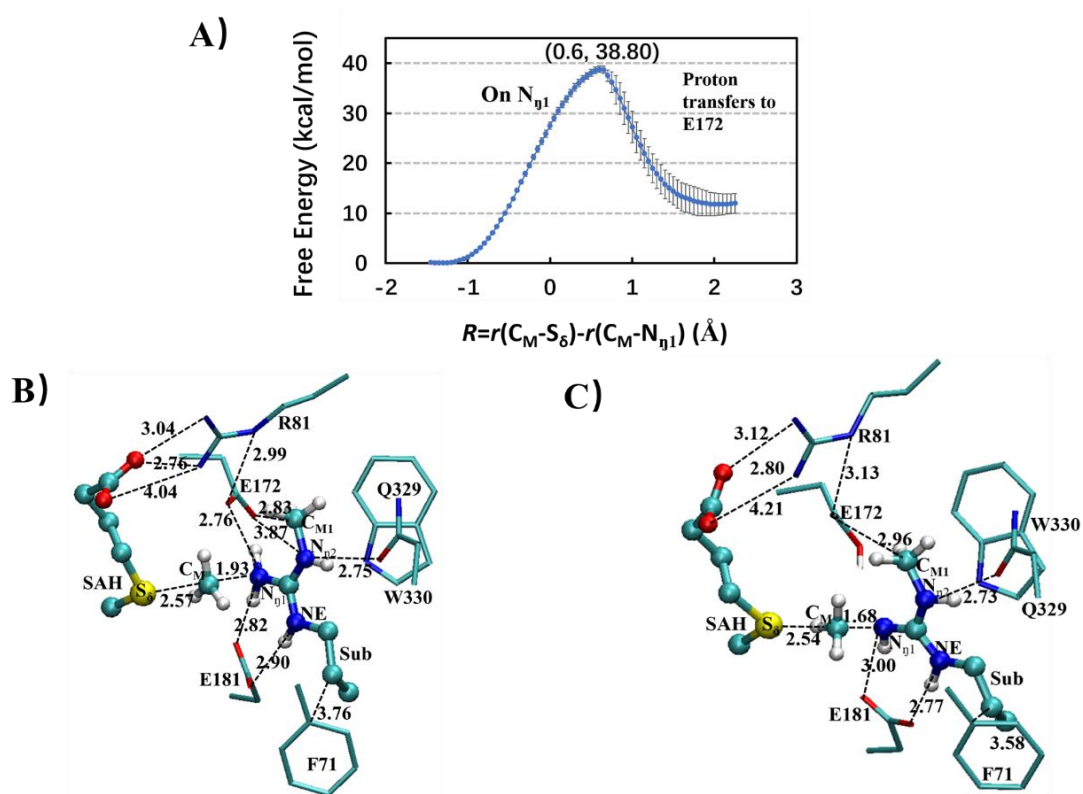


Figure S9. (A) Free energy profile for the 2nd methylation to $N_{\eta1}$ in complex III. (B) Representative active site structures of near TS for the 2nd methylation to $N_{\eta1}$ in complex III obtained from the free energy simulations. (C) Representative active site structures of (TS+2) state for the 2nd methylation to $N_{\eta1}$ in complex III obtained from the free energy simulations.

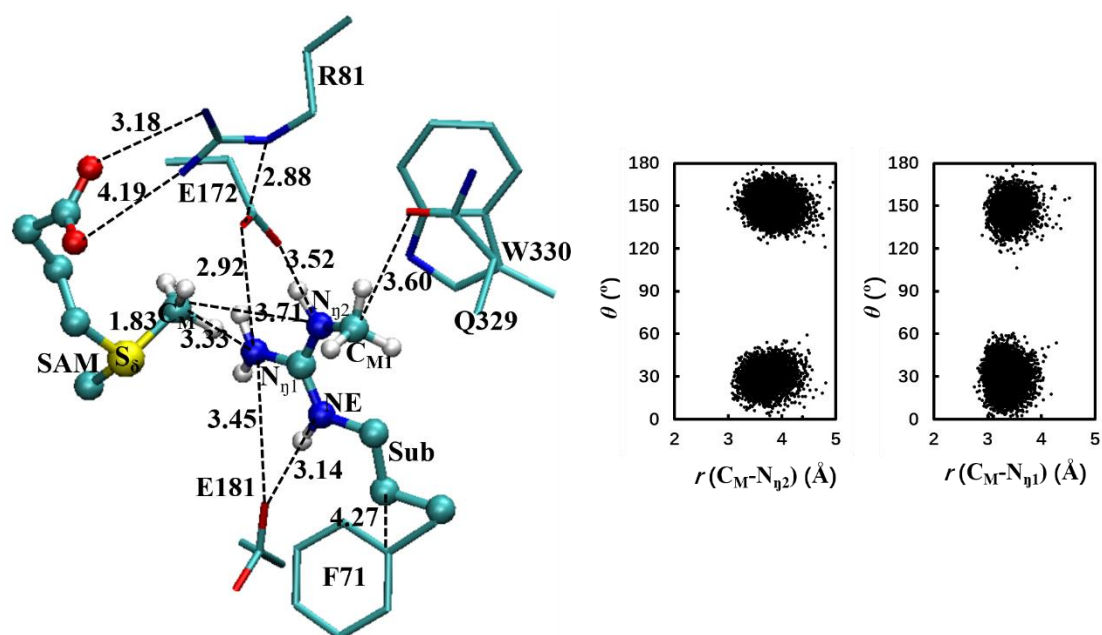


Figure S10. Representative active site structure of the reactant complex IV for 2nd methylation along with $r(\text{C}_M \cdots \text{N}_{\eta})$ and θ distributions obtained from the QM/MM simulation. (left) 2nd methylation on N_{η2}. (right) 2nd methylation on N_{η1}.

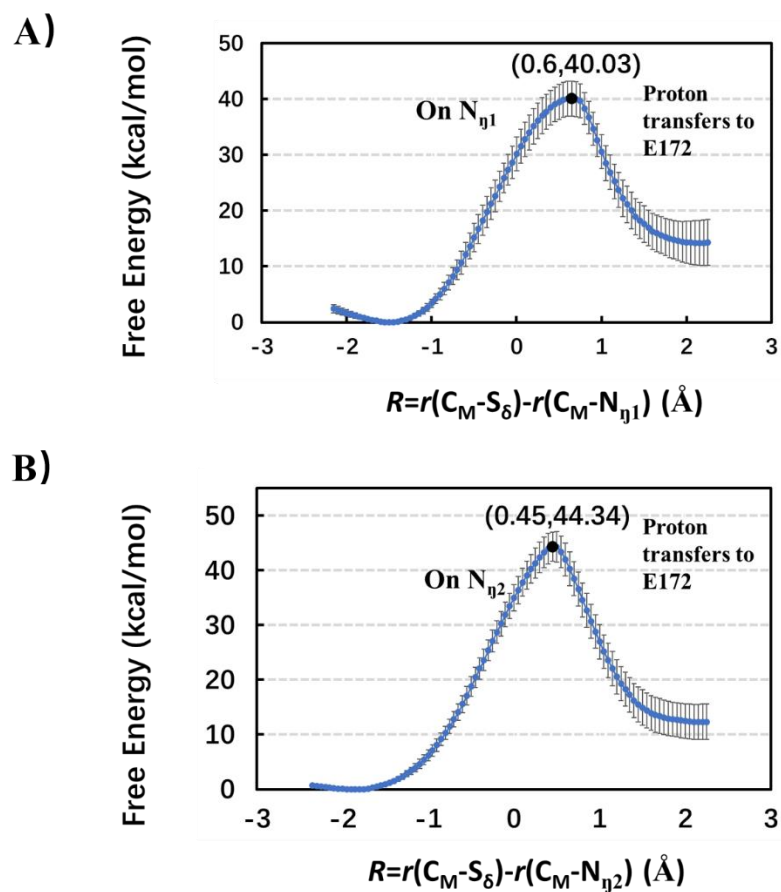


Figure S11. (A) Free energy profile for the 2nd methylation to $N_{\eta 1}$ in complex IV. (B) Free energy profile for the 2nd methylation to $N_{\eta 2}$ in complex IV.

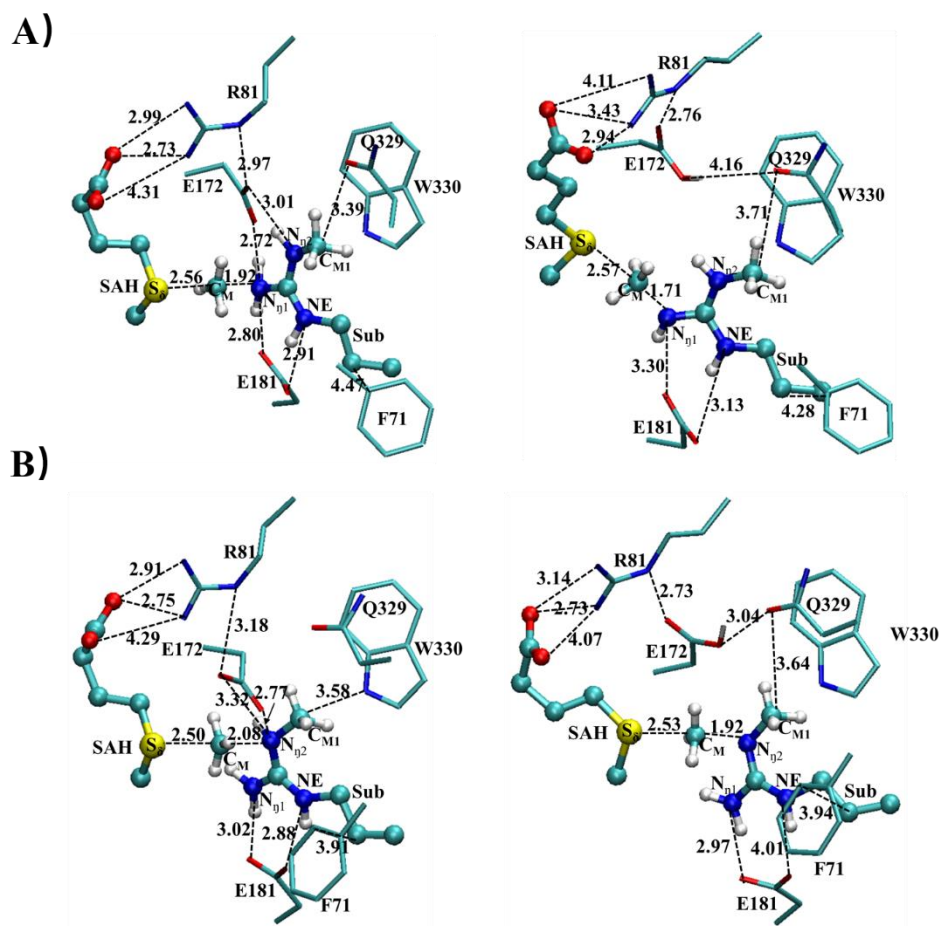


Figure S12. (A) Representative active site structures of near TS for the 2nd methylation to N_{η1} in complex IV obtained from the free energy simulations. (B) Representative active site structures of (TS+1) state for the 2nd methylation to N_{η1} in complex IV obtained from the free energy simulations. (C) Representative active site structures of near TS for the 2nd methylation to N_{η2} in complex IV obtained from the free energy simulations. (D) Representative active site structures of (TS+2) state for the 2nd methylation to N_{η2} in complex IV obtained from the free energy simulations.